

Turbulent Shear Stresses in Compressible Boundary Layers

A. J. Laderman* and Anthony Demetriades†

Ford Aerospace & Communications Corporation, Aeronutronic Division, Newport Beach, Calif.

Hot-wire anemometer measurements of turbulent shear stresses in a zero pressure gradient, two-dimensional, flat plate compressible boundary layer are described. Tests were conducted for a freestream Mach number M_e of 3, wall to freestream total temperature ratios T_w/T_{oe} of 0.94 (adiabatic) and 0.71, and Reynolds number based on momentum thickness of approximately 3500. The shear stress measurements reported here are shown to be in good agreement with the results determined indirectly from mean flow profiles obtained in the same boundary layer and with direct measurements reported by other investigators. In addition, corrected shear stresses presented for two previous investigations ($M_e = 7.1$ and 9.4) are also found to agree with expectations based on existing data sources. This finding resolves the recent controversy surrounding direct shear stress measurements at high Mach numbers. On the basis of these results, it is verified that, when expressed in the form τ/τ_w vs y/δ , the turbulent shear stress distribution across the boundary layer is invariant with Mach number and corresponds to the incompressible shear stress profile. This indicates that the absolute magnitude of τ diminishes significantly with increasing Mach number as a consequence of a similar reduction in the wall shear stress at high M_e . Furthermore, the normalized shear stress distribution is shown to be independent of wall temperature over the range of T_w/T_{oe} from 0.4 to 1.0. Finally, the effects of correcting the measured hot-wire signals for frequency response limitations of the electronic instrumentation was investigated. Results demonstrated that response restoration is essential in order to deduce the correct shear stress distribution, particularly in the vicinity of the wall.

Nomenclature

C_f	= skin friction coefficient
M	= Mach number
P	= pressure
R_{ij}	= cross-correlation coefficient of i and j fluctuations
Re_θ	= Reynolds number based on momentum thickness
T	= temperature
u	= streamwise velocity component
u_τ	= friction velocity $\equiv (\tau_w/\rho_w)^{1/2}$
v	= normal velocity component
y	= distance normal to surface
δ	= boundary-layer thickness
ρ	= density
τ	= shear stress
$\langle () \rangle$	= rms fluctuation

Subscripts

e	= boundary-layer edge condition
o	= stagnation condition
w	= wall condition

Superscripts

$()$	= mean value
$()'$	= fluctuating value

I. Introduction

NUMERICAL computation of compressible turbulent flows requires appropriate models for the turbulent transport terms which appear in the "time averaged" equations of motion. The transport properties, however, cannot be determined theoretically and there is a lack of

experimental data to model these properties adequately over a wide range of flow conditions. For example, a systematic study of the effects of heat transfer on turbulence in zero pressure gradient, compressible boundary layers has not yet been conducted, and the relatively few measurements that exist are restricted to hypersonic Mach numbers. The present task, therefore, was undertaken to determine the effects of wall cooling on the structure of turbulence in a supersonic boundary layer. This report describes the results of constant current hot-wire anemometer measurements of the turbulent fluctuations, including, in particular, the Reynolds shear stress $\rho u'v'$, carried out at Mach 3 under adiabatic and moderately cold wall conditions. A detailed description of the mean flow profiles obtained under identical test conditions has been documented in Ref. 1.

Direct experimental measurements of the Reynolds shear stress are relatively scarce. In addition to the incompressible data of Klebanoff,² Townsend,³ and Zoric,⁴ measurements for zero pressure gradient boundary layers have been reported by Horstman and Rose⁵ and Acharya⁶ for subsonic flows; Johnson and Rose,⁷ who used both the constant temperature hot-wire and laser doppler velocimetry (LDV) at Mach 3; Yanta and Lee,⁸ also using the LDV at Mach 3; Mikulla and Horstman,⁹ who used a specially designed hot-wire probe at Mach 6.8; Laderman,¹⁰ using the constant-current hot-wire at Mach 7.1; and Demetriades and Laderman,¹¹ also using the constant-current anemometer at Mach 9.4. When the turbulent shear stress τ , normalized by the wall shear τ_w , is plotted as a function of distance from the wall y , normalized by the boundary-layer thickness δ , the results of Refs. 2-4 and 7-9 are found to be insensitive to Mach number and wall temperatures. The finding is reinforced by a number of well-documented mean flow studies for Mach numbers ranging from 2 to 10 (see Refs. 12 and 13). In these cases, the turbulent shear stress distribution has been determined indirectly, assuming self-similar flow and using the measured mean flow profiles to integrate the momentum equation. The results of these calculations have been reviewed by Sandborn¹³ and, within a relatively small scatter, were found to be

Received Aug. 24, 1978; revision received Jan. 31, 1979. Copyright © American Institute of Aeronautics and Astronautics, Inc., 1979. All rights reserved.

Index categories: Supersonic and Hypersonic Flow; Boundary Layers and Convective Heat Transfer—Turbulent.

*Principal Scientist, Fluid Mechanics Department. Member AIAA.

†Supervisor, Fluid Mechanics Department. Associate Fellow AIAA.

independent of freestream and wall conditions and the momentum thickness Reynolds number Re_θ . Sandborn¹³ represented the results of the various investigations by a narrow band denoting the variation of τ/τ_w with y/δ , which he designates as the "best estimate" of the shear stress distribution for compressible, high-speed flow. It is also shown in Ref. 13 that the incompressible data of Klebanoff and Zoric agree with this "best estimate," so that a single τ/τ_w vs y/δ distribution appears valid for $M_e = 0$ to hypersonic speeds.[‡] Further, as shown in Ref. 1, when the "inverse method" is applied to the mean flow data of the present experiment, the computed shear stress distributions are in agreement with Sandborn's "best estimate."

In contrast to the preceding situation, when the results of Refs. 10 and 11 were plotted in the form τ/τ_w vs y/δ , they indicated a marked departure from Sandborn's "best estimate." In particular, the Reynolds stresses throughout the boundary layer were found to be considerably less than the wall shear, to decrease slightly with wall temperature, and to drop off rapidly with increasing Mach number. The "inverse" calculation of turbulent shear stress was not made in these cases since insufficient mean flow data were available. A direct comparison, therefore, of the measured shear stress with that extracted from mean flow measurements made in the same boundary layer was not possible.

The dilemma just described was resolved during the course of the present program. A review of the modal analysis used in the data reduction revealed an error in the expressions used in Refs. 10 and 11 to calculate the shear stresses. When the appropriate corrections are made, the results of these experiments conform with those of Refs. 2-4 and 7-9. Furthermore, the results of the present shear stress measurements at Mach 3 are also in good agreement with the previous shear stress data and lend additional support to the universality of the τ/τ_w vs y/δ distribution deduced from existing data sources.

II. The Experiment

Tests were carried out in the Aeronutronic Mach 3 wind tunnel using the flat plate model described in Ref. 1. The tunnel was operated at stagnation pressure P_o and stagnation temperature T_o of 0.973×10^5 N/M² and 318 K, respectively, corresponding to a unit freestream Reynolds number of 6.57×10^6 /m. While the mean flow measurements documented in Ref. 1 were made at x stations 35.1, 38.8, and 42.5 cm from the throat, and wall temperatures of 0.94, 0.714, and 0.54 T_o , the turbulence measurements were restricted to the 38.8 cm station and the former two wall conditions. Attempts to make turbulence measurements at $T_w/T_o = 0.54$ were unsuccessful due to excessive hot-wire failures. As reported in Ref. 1, a very thin frost layer covered the surface of the flat plate at this wall temperature and it is believed that small ice particles scrubbed from the surface by the airflow were responsible for the high failure rate of the hot wires.

The fluctuation measurements were made using hot-wire x -array probes operated in the constant current mode with wire diameters of 5.08×10^{-4} mm and aspect ratios of about 150. The vertical extent of the hot-wire element was approximately 0.05 mm corresponding to 0.5% of the boundary-layer thickness. Construction details of the hot-wire probes are given in Refs. 14 and 15, while a description of the procedure used to determine the effective angle of inclination of the

wire elements to the flow is described in Ref. 15. The hot wires were "oven calibrated" prior to the tests to determine their temperature coefficient of resistivity and "flow calibrated" during the tests to derive the heat-transfer characteristics needed to calculate the sensitivity coefficients.¹⁶ During the measurements, the hot-wire outputs were recorded on magnetic tape to create a permanent data file of the turbulence signals.

The probe was mounted in a motor-driven actuator extending through the tunnel ceiling, whose motion could be controlled to 0.025 mm as indicated by a gear-actuated counter. When positioned near the wall, the probe tip was viewed with a 10-power microscope equipped with a calibrated graticule. This permitted the wall location to be determined to within 0.025-0.05 mm.

III. Method of Analysis

The theory of the hot-wire anemometer for incompressible flow has been thoroughly documented in the literature. The application of the hot wire to supersonic flows, where compressibility effects introduce density fluctuations in addition to the usual vorticity disturbances, was successfully demonstrated by Kovaszny, Morkovin, and their co-workers (e.g., see Refs. 17 and 18), who developed the method of modal analysis to interpret the hot-wire signals. Adaptation of these techniques to the x -probe configuration has generally been restricted to the case of symmetrical, matched wires in order to simplify the governing expressions.¹⁸ In practice, however, matched wires are difficult to fabricate, particularly for the small wire diameters used in the present experiment, which offer the advantages of large signal to noise ratio and improved frequency response. Therefore, for these tests, efforts were directed toward fabrication of similar, but not necessarily, identically matched wires. The extension of the modal analysis method to the x -probe anemometer for the general case where the two hot wires comprising the probe have different characteristics and are inclined at angles other than ± 45 deg is presented in Ref. 19. The sole restriction to the method is the assumption that pressure fluctuations are negligible. An interesting feature of the analysis is that while $\langle u' \rangle$ and $\langle T' \rangle$ are uniquely determined, two solutions are provided for $u'v'$ and three results are obtained for $\langle v' \rangle$. In the interest of conserving space, this paper is restricted to a review of the numerical results for the modally resolved fluctuations and the reader interested in the details of the analysis should consult the reference cited.

As mentioned in Sec. I, the Reynolds shear stress determined in two previous studies of hypersonic boundary layers^{10,11} were incorrectly interpreted. The error arose from inadvertently extending the formulation for low-speed heated flows to the high-speed, compressible case and was caused by improper identification of the hot-wire sensitivity coefficients. These prior cases are discussed in Sec. IV, where corrected results, based on the proper method of analysis, are presented.

It should be noted that, in order to deduce the correct level of the fluctuation intensities, the frequency response of the constant current hot wire and its associated electronics must be taken into account. Because of its finite thermal capacitance, the hot-wire signal is attenuated at the higher frequencies. An attempt to restore the hot-wire output to its correct level is made by feeding the signal to a compensating circuit whose frequency response is the inverse of that of the hot wire. Exact compensation is rarely achieved since the hot-wire time constant changes with Reynolds number (y position) and overheat (current), while the compensator is set to a fixed time constant. Any attempt to make a point-by-point adjustment of the compensator to match the hot-wire time constant under all conditions would increase the labor involved in the measurements beyond practical proportions. The compensator output is then fed to an amplifier to increase

[‡]It should be pointed out that the subsonic results reported by Hortsmann and Rose⁵ and by Acharya⁶ differ somewhat from Sandborn's "best estimate" and indicate a more linear variation through the boundary layer. The reason for this difference is not clear, but since the incompressible data of Refs. 2 and 4 are in excellent agreement with the supersonic results, the subsonic data of Refs. 5 and 6 represent a significant deviation from a well-defined trend.

the hot-wire signal to a convenient level and to a tape recorder to create a permanent data file. For both the amplifier and the recorder, the response function drops below unity at the higher frequencies (up to 600 kHz) where signals are known to occur. Thus, the raw data must be corrected for the instrument limitations before proceeding with the modal analysis. Details of the response restoration procedure and its application to the present measurements have been described in Ref. 19.

IV. Results

Corrected Results for Refs. 10 and 11

Before discussing the results of the present tests, it is instructive to consider corrected results for the measurements of Refs. 10 and 11. In the former, measurements were made at AEDC Tunnel B in the boundary layer over a 4 deg semivortex angle, sharp cone at $M_e = 7.1$ and $T_w/T_{oe} = 0.4$ and 0.8, while in the latter, tests were carried out in the test section ceiling boundary layer of the two-dimensional JPL hypersonic wind tunnel at $M_e = 9.4$ and $T_w/T_{oe} = 0.38$. The new results for each experiment are described below.

Reference 10—AEDC Cone Boundary Layer

In Ref. 10, the boundary-layer thickness δ was originally defined as the y location where $u = 0.995 u_e$ and values $\delta = 0.894$ cm and 0.777 cm for $T_w/T_{oe} = 0.4$ and 0.8 were quoted. With this definition, the fluctuation intensities at the boundary-layer edge were still in excess of their freestream values. A review of the mean flow data indicated that the velocity approached its freestream value much faster than the other properties (e.g., ρ , M , T_o), that the latter reached 0.995 of their respective edge values at essentially the same y position, and that at this same y position, the fluctuation intensities decreased to the freestream levels. Thus, on this basis, the boundary-layer thickness δ was redefined and the revised values are used here to normalize the y position of the probe. In addition, direct measurements of the wall shear, needed to normalize the shear stress measurements, were not made in this experiment. Instead, based on the experimental Re_θ , the skin friction coefficient has been calculated from the von Karman-Schoenherr correlation, using the Van Driest velocity transformation as outlined in Ref. 20. The values of δ and C_f used in the reduction of data for Ref. 10 are: for $T_w/T_{oe} = 0.4$, $\delta = 1.37$ cm and $C_f = .00131$; for $T_w/T_{oe} = 0.8$, $\delta = 1.44$ cm and $C_f = .00120$. The normalized velocity fluctuations $\langle u' \rangle / \bar{u}$ and $\langle v' \rangle / \bar{u}$ are plotted vs y/δ in Fig. 1, for both the cold and adiabatic wall conditions. The rms longitudinal velocity fluctuation $\langle u' \rangle / \bar{u}$ is unchanged from the values presented in Ref. 10 and it is seen again that this quantity is insensitive to wall temperature. The corrected analysis now provides three solutions for $\langle v' \rangle / \bar{u}$ and, as plotted in Fig. 1, the mean value is represented by the symbol with the range of the maximum and minimum values denoted by the vertical bar. Because of scatter in the data at $T_w/T_{oe} = 0.8$, the effect of wall temperature on the vertical velocity fluctuation is not certain. However, the data clearly indicate that $\langle v' \rangle / \bar{u}$ is greater than $\langle u' \rangle / \bar{u}$, in contrast to the incompressible case where $\langle v' \rangle / \bar{u}$ is about 0.7 $\langle u' \rangle / \bar{u}$. This finding is supported by the data reported by Owens et al.²¹ and by Mikulla and Horstman,⁹ which were obtained at similar Mach number and wall temperature, although at higher Re_θ , as the cold wall condition of the AEDC cone experiments. Further elaboration of this point is presented later.

The results of the corrected modal analysis yield a single solution for $\langle T' \rangle / \bar{T}$, instead of the three solutions indicated in Ref. 10. However, the corrected temperature fluctuations are essentially unchanged from the previous results since they correspond to essentially an average of the values given in Ref. 10.

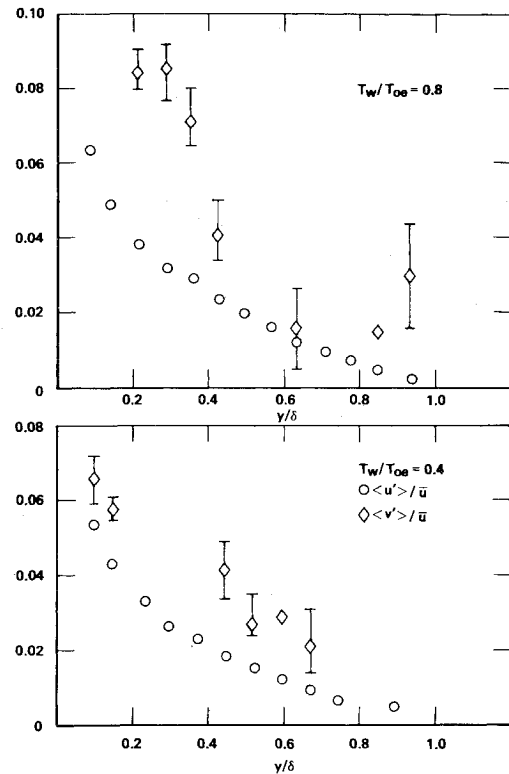


Fig. 1 Variation of velocity fluctuations across the AEDC cone boundary layer at Mach 7.1.¹⁰

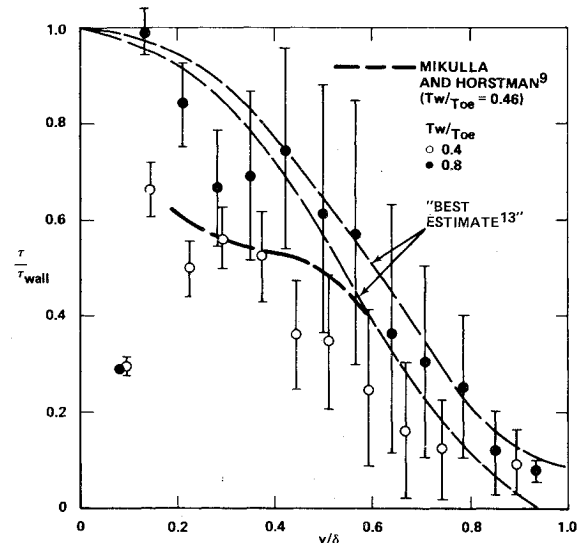


Fig. 2 Corrected turbulent shear distribution for AEDC cone boundary layer at Mach 7.1.¹⁰

The Reynolds shear stress distribution across the boundary layer, plotted in the form τ/τ_w vs y/δ , is presented in Fig. 2. The two solutions provided by the modal analysis are indicated by the end points of the vertical bars shown in the figure, while the plotted symbol represents the arithmetic mean of these two values. For the adiabatic case ($T_w/T_{oe} = 0.8$), the measured shear stresses are in good agreement with the "best estimate" suggested by Sandborn.¹³ The data for the cold wall case, $T_w/T_{oe} = 0.4$, are slightly smaller than the adiabatic results, but are in good accord with the stresses reported by Mikulla and Horstman⁹ for essentially the same conditions of edge Mach number and wall temperature. For both wall conditions, the shear stress undergoes a sudden drastic reduction in magnitude near the

wall, a feature common to all other measurements obtained either with hot wires or the laser doppler velocimeter. In interpreting the results of Fig. 2, however, it should be emphasized that for this test the data analysis was carried out without response restoration to the hot-wire signals. The significance of the response restoration procedure, in particular its effects on data acquired near the wall, is illustrated later when the results of the present Mach 3 measurements are described. Even in the absence of signal restoration, it is clear from Fig. 2 that the measurements of Ref. 10 have now been brought into agreement with expectations based on data accumulated in flows ranging from subsonic to hypersonic speeds.

Ref. 11—JPL HWT Ceiling Boundary Layer

Two hot-wire x-probes, numbered 4 and 11, were used in this experiment and the results obtained with both probes are presented. The rms velocity fluctuations $\langle u' \rangle / \bar{u}$ and $\langle v' \rangle / \bar{u}$ and the rms temperature fluctuation $\langle T' \rangle / \bar{T}$ are plotted vs y/δ in Fig. 3, where again the end points of the vertical bar represent the minimum and maximum of the three solutions for $\langle v' \rangle / \bar{u}$ and the symbol denotes the arithmetic average. While there is slightly greater scatter in the results obtained from probe 11, the trends and magnitudes indicated by the two probes are in reasonable agreement. It should be noted that while $\langle u' \rangle / \bar{u}$ continues to increase as the wall is approached, $\langle v' \rangle / \bar{u}$ first increases with decreasing y/δ , then, when $y/\delta < 0.5$, decreases toward the wall. It is also seen that again $\langle v' \rangle / \bar{u}$ is greater than $\langle u' \rangle / \bar{u}$ and that $\langle v' \rangle / \langle u' \rangle$ is now greater than observed in the corrected AEDC cone results described earlier. This implies that the anisotropy of the flow is sensitive to the Mach number and becomes excessive at high speeds.

Since the wall shear stress was not measured in Ref. 11, the skin friction coefficient was determined by curve-fitting the

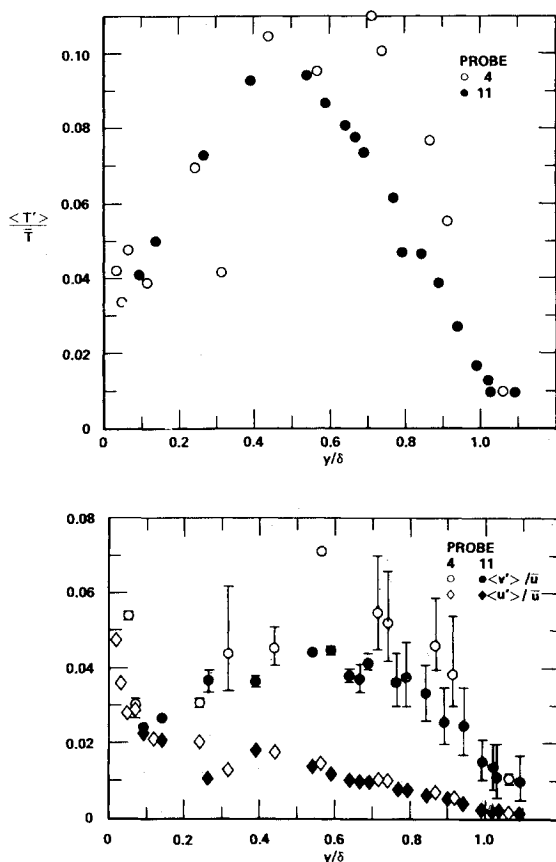


Fig. 3 Velocity and temperature fluctuations in JPL ceiling boundary layer at Mach 9.4.¹¹

measured mean velocity profile to the Coles "law-of-the-wake"²² correlation. In this procedure (see, e.g., Ref. 1), C_f is one of three adjustable boundary-layer parameters whose value is specified when the rms error in the curve-fit is minimized. From Ref. 16 then, $C_f = 0.00041$ while δ is 10 cm. Corrected Reynolds shear stress distribution, normalized by the wall shear, are shown in Fig. 4, where again the vertical bars depict the minimum and maximum values provided by the modal analysis and the symbol represents the arithmetic average. While there is considerable scatter for probe 11, the results for both probes 4 and 11 are similar for $y/\delta > 0.5$ and tend to follow the "best estimate" of Sandborn. For $y/\delta < 0.5$, the results of both probes exhibit the characteristic fall-off observed in other measurements. The scatter in these data is attributed primarily to the severity of the test environment. Since the total temperature was 810 K, it was necessary to restrict the overheat range in order to avoid excessive probe failures and this, in turn, influenced the probe sensitivity. The drop-off in τ/τ_w below $y/\delta = 0.5$ is believed to be due to the absence of response restoration. As mentioned earlier, the importance of response restoring the hot-wire signals is demonstrated in the next section.

Results of the Present Mach 3 Measurements

The shear stress measurements in the Mach 3 boundary layer described in this report have been analyzed using both unrestored and response-restored hot-wire signals. The response restoration was found to have only a minor effect on the velocity and temperature fluctuations. However, for the shear stresses, the corrections are sufficiently large that response restoration must be included in order to deduce the correct variation of τ/τ_{wall} across the boundary layer.

For the adiabatic wall temperature, the rms temperature and longitudinal velocity fluctuations are shown in Fig. 5 and the vertical velocity fluctuations are presented in Fig. 6 for both the unrestored and restored cases. Again, the minimum and maximum values of the three solutions for $\langle v' \rangle / \bar{u}$ are indicated by the end points of the vertical bars in Fig. 6 and the plotted symbol represents the arithmetic average. For each fluctuation term, it is seen that the effect of response restoration increases as the wall is approached. The largest correction due to restoring the signals occurs for the temperature fluctuations near the wall (20-30%), while for the velocity fluctuations, the corrections appear to be negligible for $y/\delta > 0.2$. Similar effects of response restoration were found for the cold wall condition $T_w = 0.71 T_{oe}$. It should also be noted that similar to the high Mach number results

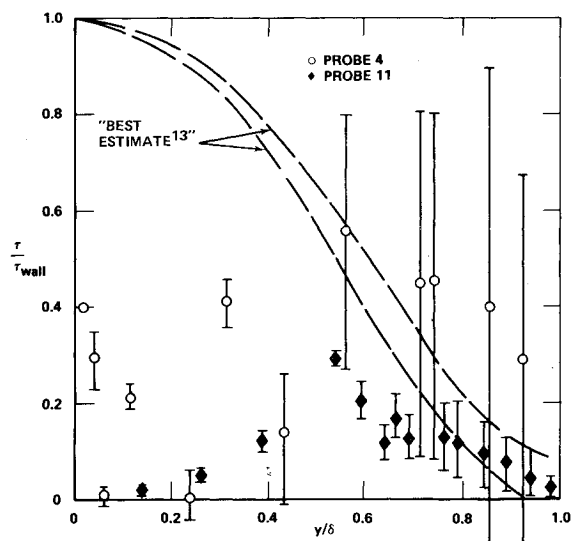


Fig. 4 Corrected turbulent shear stress distribution for JPL boundary layer at Mach 9.4.¹¹

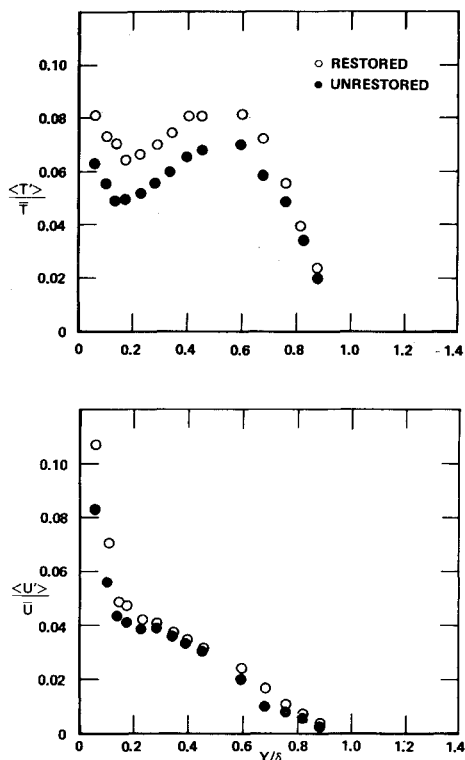


Fig. 5 Temperature and longitudinal velocity fluctuations in adiabatic wall Mach 3 boundary layer showing effect of response restoration.

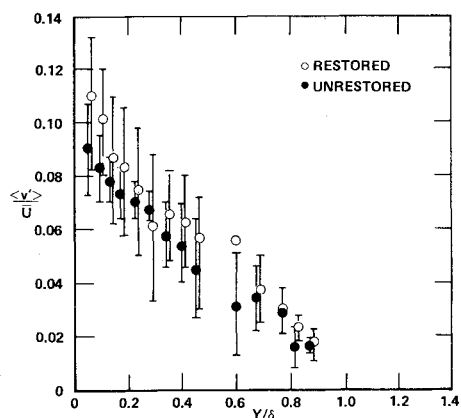


Fig. 6 Vertical velocity fluctuations in adiabatic wall Mach 3 boundary showing effect of response restoration.

described earlier, $\langle v' \rangle / \bar{u}$ is greater than $\langle u' \rangle / \bar{u}$ throughout the boundary layer.

The shear stress distribution, τ/τ_w vs y/δ for the adiabatic case, is shown in Fig. 7 which includes, for comparison, Sandborn's "best estimate" and the results of the "inverse" calculations, based on the mean flow profiles from Ref. 1. The values of skin friction coefficient C_f and boundary-layer thickness δ , for the Mach 3 boundary layer, which were determined in Ref. 1, are, respectively, 0.00196 and 0.899 cm for $T_w/T_{oe} = 0.94$, and 0.00215 and 0.856 cm for $T_w/T_{oe} = 0.71$. For the unrestored case, the turbulent shear stresses increase from zero at the boundary-layer edge and reach a peak at $y/\delta \approx 0.3$, then decrease again as the wall is approached. However, when the signals are response restored, the measured shear stress distribution closely follows both the "inverse" results from Ref. 1 and Sandborn's "best estimate" and, with the one exception at $y/\delta = 0.06$, tends toward the wall shear as y/δ decreases. Note,

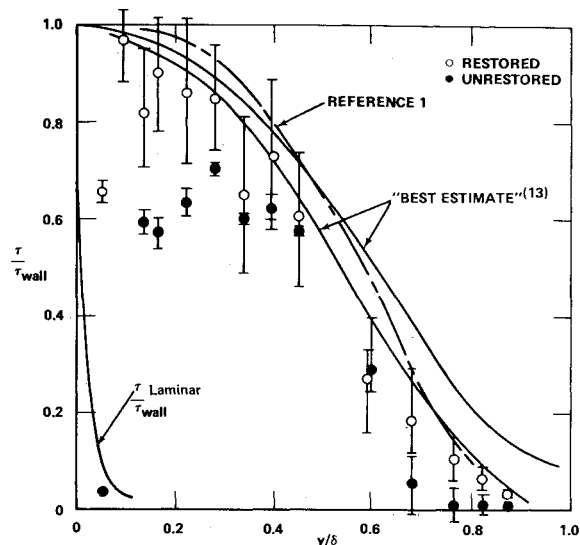


Fig. 7 Adiabatic wall turbulent shear stress distribution in Mach 3 boundary layer showing effect of response restoration.

for example, that $\tau/\tau_{wall} = 0.97$ at $y/\delta = 0.1$. Consequently, the drop-off in turbulent shear stress that has been observed with hot-wire probes (but was not detected from "inverse" calculations using measured mean flow properties), is almost completely eliminated when the hot-wire signals are corrected for response limitations of the measuring electronics. In a recent paper, Sandborn²³ attributes the drop-off in shear stress near the wall to the effects of the mean velocity gradient over the finite length of the hot-wire element and present data for a low-speed flow where the uncertainty in the velocity is 10% of the local value. In the present experiment, however, the velocity uncertainty introduced by the probe size is less than 1% for $y/\delta > 0.1$. Therefore, this cannot account for the behavior of the unrestored results for $y/\delta < 0.3$. It is concluded that response restoration of the hot-wire signals must be carried out to determine the correct variation of shear stress across the boundary layer. The relative effect of the restoration procedure will depend on the particular boundary-layer flow and is a function of the variation of Reynolds number and Mach number normal to the surface. The effects cannot be assessed a priori, however, but can be evaluated only after the required experimental data have been acquired.

The effect of wall temperature on the temperature and velocity fluctuations is shown in Fig. 8, where $\langle T' \rangle / \bar{T}$ and $\langle u' \rangle / \bar{u}$ have been plotted vs y/δ , and in Fig. 9, where the $\langle v' \rangle / \bar{u}$ distribution is presented. In both figures, only the response-restored results are shown. For the limited temperature range considered, the wall condition has relatively little influence on $\langle u' \rangle$ and $\langle v' \rangle$, although, as expected, there is a slight reduction in $\langle T' \rangle$ as the wall temperature is reduced. The turbulent shear stress distribution for the cold wall case $T_w = 0.71 T_{oe}$ is shown in Fig. 10 which includes the results of both the unrestored and restored data analyses. The trend of the shear stress distribution and the magnitude of the correction introduced by response restoration is similar to that observed in Fig. 10 for the adiabatic wall. Again, it is clear that response restoration must be included in order to deduce the corrected shear stress distribution near the wall. Note that the restored shear stress distribution is in good agreement with the results of Refs. 1 and 13.

V. Discussion

Prior to the present investigation, the limited data available for cold wall measurements of the turbulent shear stresses made the influence of wall temperature uncertain, although the "inverse" calculations of the stresses indicated the effect was small. The present direct measurements at $T_w/T_{oe} = 0.94$

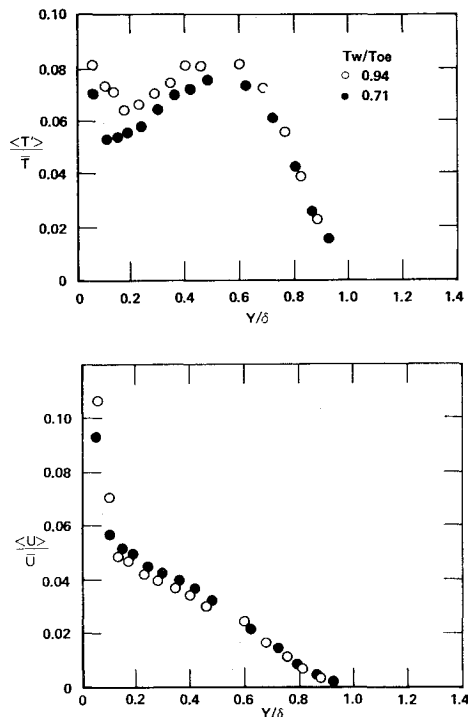


Fig. 8 Response-restored distributions of temperature and longitudinal velocity fluctuations showing effect of wall temperature.

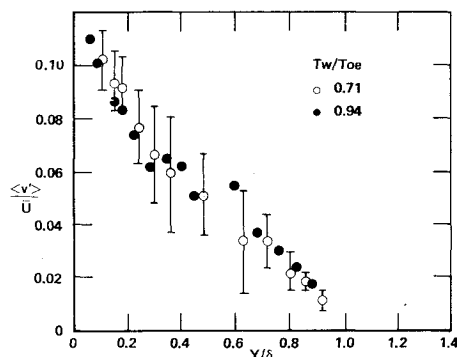


Fig. 9 Response-restored distribution of vertical velocity fluctuations showing effect of wall temperature.

and 0.714 and the "inverse" calculations for Ref. 1, which also include data for $T_w/T_{oe}=0.54$, indicate quite clearly that, when properly normalized, the turbulent stresses are unaffected by wall temperature. This conforms to the same behavior exhibited by the skin friction coefficient C_f , which is known to be only weakly dependent on heat transfer. As shown in Ref. 1, for the same external stream conditions, C_f increases only 10% as the wall temperature is reduced by a factor of 2. It is concluded, therefore, that when expressed in the form τ/τ_w vs y/δ , the turbulent shear stress distribution is independent of freestream Mach number, at least over the range 0-10, and of heat transfer, for wall temperature ratios ranging from 0.4-1.0. However, the earlier contention¹¹ that there is a rapid decrease in $u'v'$ with increasing Mach number is still valid, although the drop-off in $u'v'$ is now associated with the large reduction in wall friction at high M_e .

To further assess the present measurements, the temperature and velocity fluctuations are compared to the results of other investigations. The distribution of temperature fluctuations across the boundary layer for both $T_w/T_{oe}=0.94$ and 0.74 are plotted in Fig. 11, where they are compared to Kistler's²⁴ adiabatic results at $M_e=1.72$ and 3.56. The present adiabatic results are seen to be slightly smaller than

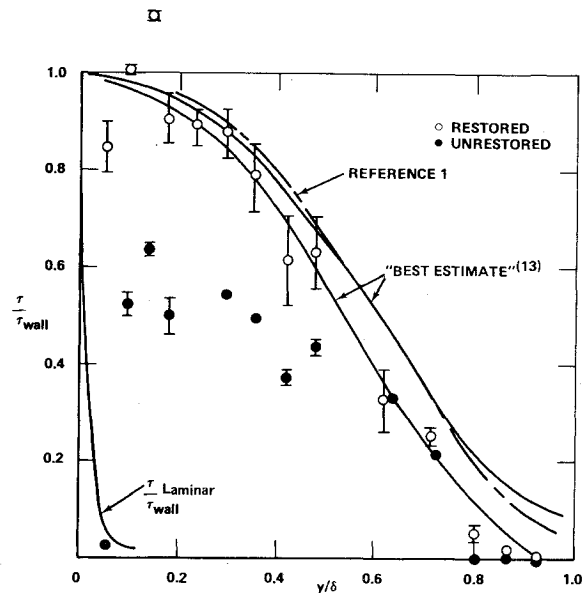


Fig. 10 Turbulent shear stress distribution across the boundary layer for Mach 3 and $T_w/T_{oe}=0.71$ showing effect of response restoration.

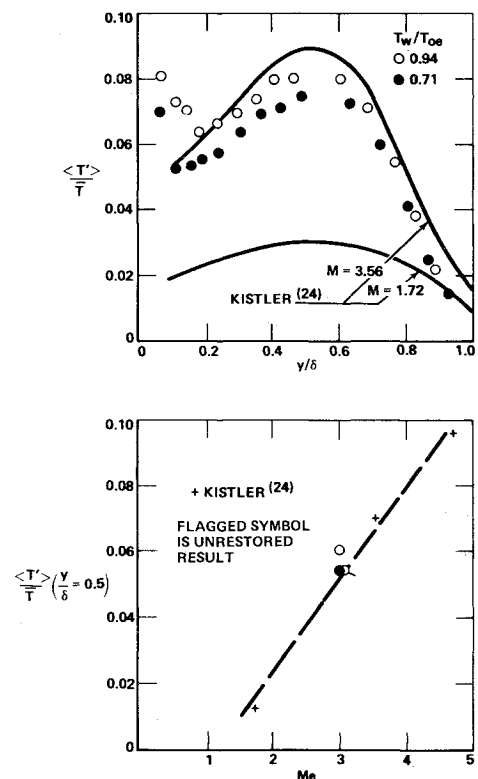


Fig. 11 Comparison of temperature fluctuation in Mach 3 boundary layer to Kistler's results.²⁴

Kistler's data at $M_e=3.56$. The comparison between the two sets of data becomes more obvious when $\langle T' \rangle / \bar{T}$ at $y/\delta=0.5$ is plotted against Mach number as shown in Fig. 11. Here, the present Mach 3 result is approximately 10% greater than that expected on the basis of Kistler's measurements. It should be noted, however, that Kistler's data are not response-restored. Thus, if the unrestored result for the present experiment is plotted in Fig. 11, it is seen to agree quite closely to the value interpolated from Kistler's results.

At least a dozen measurements of $\langle u' \rangle$ have been reported for a wide range of Mach numbers, wall temperatures, and Re_θ . Rather than compare the entire distribution of velocity

REFERENCE	AUTHOR	Me	Tw	Reg
2	○ KLEBANOFF	0	To	500 - 7,000
3	○ TOWNSEND	0	To	600
6	▽ ACHARYA	0.2 - 0.6	To	2,000 - 3,500
18	▲ MORKOVIN	1.72	To	17,000
8	● YANTA AND LEE	3	To	13,000
24	○ KISTLER	1.7 - 4.7	To	28,000 - 40,000
7	△ JOHNSON AND ROSE	3	To	74,000
26	* ROSE	3.9	To	5,000
21	■ OWEN ET AL	6.8	0.46 To	7,300
9	⊙ MIKULLA AND HORSTMAN	6.8	0.46 To	7,300
10	△ LADERMAN	7.1	0.8 To	1,400
10	△ LADERMAN	7.1	0.4 To	2,000
27	□ LADERMAN AND DEMETRIADES	7.2	0.8 To	1,000 - 5,000
11	◆ DEMETRIADES AND LADERMAN	9.4	0.38 To	37,000
	◇ PRESENT MEAS	3	0.94 To	3,500
	◆ PRESENT MEAS	3	0.71 To	3,500

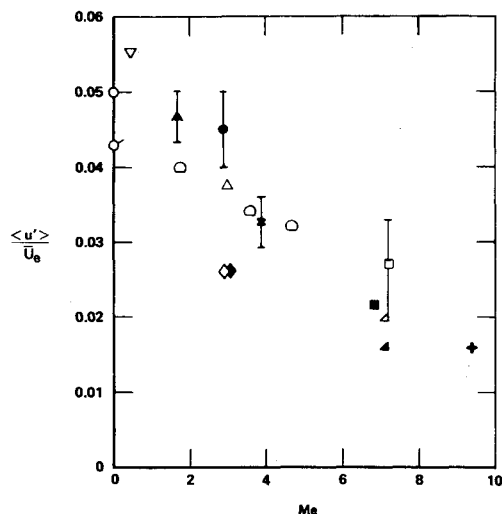


Fig. 12 Variation of longitudinal velocity fluctuations at $y/\delta=0.5$ with edge Mach number.

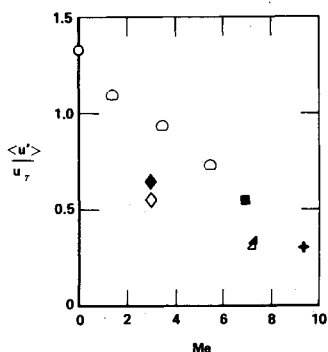


Fig. 13 Correlation of longitudinal velocity fluctuations. (See Fig. 12 for legend.)

fluctuations across the boundary layer, for clarity, a single point located at the midpoint of the boundary layer was selected as representative of the fluctuations for each test condition. A plot of $\langle u' \rangle / \bar{u}_e$ at $y/\delta=0.5$ vs Me is shown in Fig. 12. While there is some scatter in the data, it is clear that $\langle u' \rangle / \bar{u}_e$ tends to decrease as Me increases. Although most of the results shown in Fig. 12 were obtained assuming $\langle p' \rangle = 0$, it is well known that the pressure fluctuations increase with increasing Mach number. However, the effect of $\langle p' \rangle$ on temperature and velocity fluctuations was examined in Ref. 16, where the modal analysis was carried out both for $\langle p' \rangle = 0$ and for finite $\langle p' \rangle$, and it was found that the rms fluctuations $\langle T' \rangle$ and $\langle u' \rangle$ were relatively unaffected by whether or not $\langle p' \rangle$ was included. Since this test was applied to the high Mach number data point ($Me=9.4$) in Fig. 12, which conforms to the trend exhibited by the remaining data, it is concluded that the data provide a valid estimate of the variation of $\langle u' \rangle / \bar{u}$ with edge Mach number. A more revealing picture is indicated in Fig. 13, where $\langle u' \rangle$ normalized by u_t is plotted vs Me . Again, the trend of decreasing velocity fluctuations with increasing Me is observed and, in addition, it appears that the velocity fluctuations for the present tests are 50% less than expected from the previous

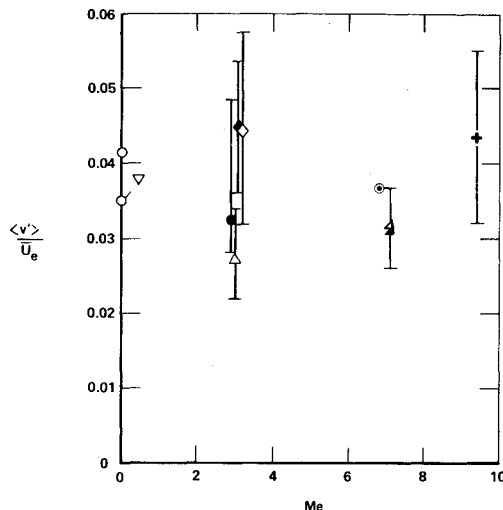


Fig. 14 Variation of vertical velocity fluctuations at $y/\delta=0.5$ with edge Mach number. (See Fig. 12 for legend.)

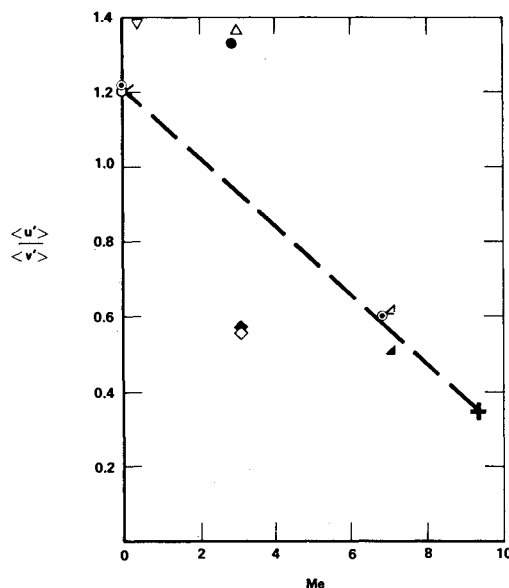


Fig. 15 Variation of $\langle u' \rangle / \langle v' \rangle$ at $y/\delta=0.5$ with edge Mach number. (See Fig. 12 for legend.)

data. Morkovin²⁵ suggested that the velocity fluctuations could be correlated by multiplying $\langle u' \rangle / u_t$ by a density stretching coordinate $(\rho/\rho_w)^{1/2}$. Based on the data shown in Fig. 13, it was found that the Morkovin correlation is valid only for $Me < 4$. These conclusions, however, are provisional because of the $p'=0$ assumption just mentioned, and especially since the high Me data were not accompanied by simultaneous wall friction measurements.

The vertical velocity fluctuations $\langle v' \rangle / \bar{u}_e$ at $y/\delta=0.5$ are plotted vs Me in Fig. 14. Although the scatter in the measurements is larger than for $\langle u' \rangle / \bar{u}_e$, it is clear that $\langle v' \rangle / \bar{u}_e$ is relatively independent of Mach number. This is a significant finding since it indicates that the flow becomes highly anisotropic at high Mach numbers with $\langle v' \rangle$ exceeding $\langle u' \rangle$. This is demonstrated in Fig. 15 where $\langle u' \rangle / \langle v' \rangle$ has been plotted vs Me . (The data scatter shown in Fig. 14 has been omitted in Fig. 15 since it becomes highly exaggerated when the data are plotted in the form $\langle u' \rangle / \langle v' \rangle$.) The dashed line in Fig. 15 was arbitrarily drawn through the incompressible and high Mach number data and serves to confirm that the $\langle u' \rangle$ of the present tests is low and, furthermore, indicates that the $\langle v' \rangle$ data of Refs. 7 and 8 is also low.

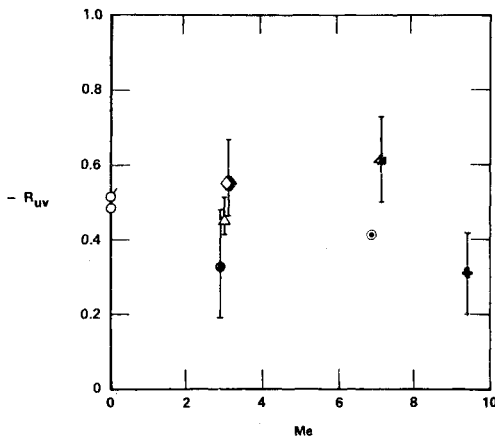


Fig. 16 Velocity cross-correlation R_{uv} at $y/\delta=0.5$ as a function of edge Mach number. (See Fig. 12 for legend.)

A final plot is shown in Fig. 16 where R_{uv} at $y/\delta=0.5$ is plotted vs M_e . It is difficult to draw any firm conclusions from Fig. 16 since the scatter and uncertainty in the data are relatively large. However, it appears that R_{uv} is independent of both Mach number and wall temperature and is approximately 0.5.

VI. Summary

1) The measured turbulent shear stress distribution for the Mach 3 boundary layer have been shown to be in good agreement with those obtained from integration of the mean flow profiles presented in Ref. 1. In addition, these results, together with the corrected shear stresses for Ref. 10 (AEDC cone boundary layer at $M_e=7.1$) and 11 (JPL HWT wall boundary layer at $M_e=9.4$) are in good accord with those obtained from other investigations. These findings serve to clarify finally the effects of compressibility and heat transfer on the turbulent shear stresses in a two-dimensional, zero pressure gradient boundary layer. There are now sufficient direct stress measurements to support Sandborn's¹³ earlier contention, based primarily on indirect evidence, that when expressed in the form τ/τ_w vs y/δ , the shear stress distribution is essentially independent of Mach number and heat transfer. This conclusion appears valid for Mach numbers ranging from incompressible to hypersonic speeds and T_w/T_{oe} ranging from 0.4 to 1.0. It should be clear, however, that since the wall shear undergoes a significant decrease with increasing M_e , there is a corresponding reduction in the absolute magnitude of τ at high Mach numbers.

2) Corrections to the measured hot-wire signals which account for frequency-response limitations of the instrumentation, has been demonstrated to be an essential ingredient in the data reduction process. Using response-restored signals in the present case, the drop-off in shear stress near the wall, common to almost all measurements, vanishes and the turbulent stress tends uniformly to the wall value as the surface is approached. Interestingly enough, the response restoration for the Mach 3 boundary layer had only a minor influence on the temperature fluctuations and, particularly, on the velocity fluctuations. For a given boundary layer, however, the relative effect of response restoration will depend on the variation in mean flow properties across the layer and the response characteristics of the electronics.

3) The longitudinal velocity fluctuations $\langle u' \rangle / \bar{u}_e$ for the present Mach 3 tests were found to be approximately 50% less than that expected on the basis of the available data base. Scaling the fluctuations for Re_θ and compressibility effects failed to improve the comparison, and the reason for the discrepancy is not known. However, the distribution and magnitude of the temperature fluctuations $\langle T' \rangle / \bar{T}$ were

found to be in excellent agreement with Kistler's results²⁴ based on his measurements for Mach numbers ranging from 1.72-4.76. Similarly, the vertical velocity fluctuations compare favorably with the limited data available which indicates that $\langle v' \rangle / \bar{u}_e$ is unaffected by wall temperature and independent of Mach number for $M_e=0-10$. In addition, the existing data indicate that $\langle u' \rangle / \langle v' \rangle$ decreases significantly with increasing Mach number. The highly anisotropic flow at high M_e is characterized by $\langle v' \rangle$ much larger than $\langle u' \rangle$ in contrast to incompressible flow where $\langle v' \rangle \sim 0.7$ or $0.8 \langle u' \rangle$.

Acknowledgment

This work was supported by the U.S. Army Office of Scientific Research and NASA, Moffett Field, Calif., under Contract DAAG29-75-C-0014.

References

- Laderman, A. J., "Effect of Wall Temperature on a Turbulent Supersonic Boundary Layers," *AIAA Journal*, Vol. 16, July 1978, pp. 723-729.
- Klebanoff, P. S., "Characteristics of Turbulence in a Boundary Layer with Zero Pressure Gradient," NACA TR 1247, 1955.
- Townsend, A. A., "The Structure of Turbulent Shear Flow," Cambridge University Press, Cambridge, Mass., 1956.
- Zoric, D. L., "Approach of Turbulent Boundary Layer to Similarity," Ph.D. Dissertation, Colorado State University, Rept. CER-69DLZ9, 1968.
- Horstman, C. C. and Rose, W. G., "Hot Wire Anemometry in Transonic Flow," NASA TMX-60495, Dec. 1975.
- Acharya, M., "Effects of Compressibility on Boundary Layer Turbulence," AIAA Paper 76-334, 1976.
- Johnson, D. A. and Rose, W. C., "Measurements of Turbulence Transport Properties in a Supersonic Boundary Layer Flow Using Laser Velocimeter and Hot Wire Anemometer Techniques," AIAA Paper 73-1045, 1973; also *AIAA Journal*, Vol. 13, April 1975, pp. 512-515.
- Yanta, W. J. and Lee, R. E., "Determination of Turbulence Transport Properties with the Laser Doppler Velocimeter and Conventional Time-Averaged Mean Flow Measurements at Mach 3," AIAA Paper 74-575, 1974; also *AIAA Journal*, Vol. 14, June 1976, pp. 725-729.
- Mikulla, V. and Horstman, C. C., "The Measurement of Shear Stress and Total Heat Flux in a Non-Adiabatic Turbulent Hypersonic Boundary Layer," AIAA Paper 75-119, Pasadena, Calif., Jan. 1975.
- Laderman, A. J., "New Measurements of Turbulent Shear Stresses in Hypersonic Boundary Layers," *AIAA Journal*, Vol. 14, Sept. 1976, pp. 1286-1291.
- Demetriades, A. and Laderman, A. J., "Reynolds Stress Measurements in a Hypersonic Turbulent Boundary Layer," *AIAA Journal*, Vol. 11, Nov. 1973, pp. 1594-1596.
- Bushnell, D. M. and Morris, D. J., "Shear Stress, Eddy-Viscosity, and Mixing Length Distributions in Hypersonic Turbulent Boundary Layers," NASA TMX-2310, 1971.
- Sandborn, V. A., "A Review of Turbulence Measurements in Compressible Flow," NASA TM X-62337, March 1974.
- Doughman, E. L., "Development of a Hot Wire Anemometer for Hypersonic Turbulent Flows," *Rev. Sci. Instr.*, Vol. 43, No. 8, 1972, p. 1200.
- Demetriades, A., "Final Technical Report, Advanced Penetration Program III," SAMSO TR 72-161, April 1972.
- Laderman, A. J. and Demetriades, A., "Mean and Fluctuating Flow Measurements in the Hypersonic Boundary Layer Over a Cooled Wall," *Journal of Fluid Mechanics*, Vol. 63, Pt. 1, March 1974, pp. 121-144.
- Kovaszny, L. S. G., "Turbulence in Supersonic Flow," *Journal of the Aeronautical Sciences*, Vol. 20, No. 10, 1973, p. 657; also *Journal of the Aeronautical Sciences*, Vol. 17, 1950, p. 565.
- Morkovin, M. V. and Phinney, R. E., "Extended Applications of Hot Wire Anemometry to High Speed Turbulent Boundary Layers," AFOSR TN-58-469 and ASTIA AD-158-279, June 1958.
- Laderman, A. J., "Final Technical Report, Effects of Mach Number and Heat Transfer on Reynolds Shear Stresses in Compressible Boundary Layers," Aeronutronic Publication U-6412, Ford Aerospace & Communications Corp., Aeronutronic Division, Newport Beach, Calif., April 1978.

²⁰Hopkins, E. J. and Inouye, M., "An Evaluation of Theories for Predicting Turbulent Skin Friction and Heat Transfer on Flat Plates at Supersonic and Hypersonic Speeds," *AIAA Journal*, Vol. 9, June 1971, pp. 993-1003.

²¹Owen, F. K., Horstman, C. C., Kussoy, M. K., "Mean and Fluctuating Flow Measurements of a Fully Developed, Non-Adiabatic, Hypersonic Boundary Layer," *Journal of Fluid Mechanics*, Vol. 70, Pt. 2, 1975, pp. 393-413.

²²Coles, D. E., "The Young Person's Guide to the Data." *Proceedings AFOSR IFP-Stanford Conference On Computation of Turbulent Boundary Layers*, Vol. 2, edited by P. E. Coles and E. A. Horst, Stanford University, 1969.

²³Sandborn, V. A., "Effect of Velocity Gradient on Measurements of Turbulent Shear Stress," *AIAA Journal*, Vol. 14, March 1976, pp. 400-402.

²⁴Kistler, A. L., "Fluctuation Measurements in a Supersonic Turbulent Boundary Layer," *The Physics of Fluids*, Vol. 2, No. 3, June 1959, p. 290.

²⁵Morkovin, M. V., "Effects of Compressibility on Turbulent Flows," *Mechanique de la Turbulence*, Colloques International du CNRS, No. 108, 1962.

²⁶Rose, W. C., "Turbulence Measurements in a Compressible Boundary Layer," *AIAA Journal*, Vol. 12, Aug. 1974, p. 1060.

²⁷Laderman, A. J. and Demetriades, A., "Turbulent Fluctuations in the Hypersonic Boundary Layer Over an Adiabatic Cone," *The Physics of Fluids*, Vol. 19, March 1976, pp. 359-361.

From the AIAA Progress in Astronautics and Aeronautics Series . . .

SATELLITE COMMUNICATIONS: FUTURE SYSTEMS-v. 54 ADVANCED TECHNOLOGIES-v. 55

Edited by David Jarett, TRW, Inc.

Volume 54 and its companion Volume 55, provide a comprehensive treatment of the satellite communication systems that are expected to be operational in the 1980's and of the technologies that will make these new systems possible. Cost effectiveness is emphasized in each volume, along with the technical content.

Volume 54 on future systems contains authoritative papers on future communication satellite systems in each of the following four classes: North American Domestic Systems, Intelsat Systems, National and Regional Systems, and Defense Systems. **A significant part of the material has never been published before.** Volume 54 also contains a comprehensive chapter on launch vehicles and facilities, from present-day expendable launch vehicles through the still developing Space Shuttle and the Intermediate Upper Stage, and on to alternative space transportation systems for geostationary payloads. All of these present options and choices for the communications satellite engineer. The last chapter in Volume 54 contains a number of papers dealing with advanced system concepts, again treating topics either not previously published or extensions of previously published works.

Volume 55 on advanced technologies presents a series of new and relevant papers on advanced spacecraft engineering mechanics, representing advances in the state of the art. It includes new and improved spacecraft attitude control subsystems, spacecraft electrical power, propulsion subsystems, spacecraft antennas, spacecraft RF subsystems, and new earth station technologies. Other topics are the relatively unappreciated effects of high-frequency wind gusts on earth station antenna tracking performance, multiple-beam antennas for higher frequency bands, and automatic compensation of cross-polarization coupling in satellite communication systems.

With the exception of the first "visionary" paper in Volume 54, all of these papers were selected from the 1976 AIAA/CASI 6th Communication Satellite Systems Conference held in Montreal, Canada, in April 1976, and were revised and updated to fit the theme of communication satellites for the 1980's. These archive volumes should form a valuable addition to a communication engineer's active library.

Volume 54, 541 pp., 6×9, illus., \$19.00 Mem., \$35.00 List
Volume 55, 489 pp., 6×9, illus., \$19.00 Mem., \$35.00 List
Two-Volume Set (Vols. 54 and 55), \$55.00 Mem. & List

TO ORDER WRITE: Publications Dept., AIAA, 1290 Avenue of the Americas, New York, N. Y. 10019